



Total gaseous mercury levels in the vicinity of the Central Mexico mountain mining zone and its dispersion area

Rocío García-Martínez¹ · Gilberto Hernández-Silva² · Rubén Pavia-Hernández¹ · Benedetto Schiavo⁵ · Miguel Flores-Espinosa³ · Ann Wellens⁴ · Ricardo Torres-Jardon¹ · Agustín Garcia-Reynoso¹ · Amparo Martínez-Arroyo^{1,6} · Arturo Gavilán-García⁶ · Luis G. Ruíz-Suárez^{1,6}

Received: 18 September 2020 / Accepted: 20 July 2021 / Published online: 7 September 2021
© The Author(s), under exclusive licence to Springer Nature B.V. 2021

Abstract

Mercury emitted to the atmosphere has a long residence time (up to a year) and can travel long distances before being deposited to land or ocean surfaces. The objective of this study were to evaluate the total gaseous mercury (TGM) ambient levels in the San Joaquín, Querétaro, mining region and to observe whether the TGM emissions from mining activity impact other regions of the country due to its dispersion. TGM was measured using an automatic Tekran model 2537A air mercury analyzer; the monitoring was carried out during March, April, and May 2015. From the ambient measurements carried out, the 8-h average concentrations range from 67 to 74 ng/m³, while the monthly averages for these three months were from 40 to 41 ng/m³ (1.3 ± 0.4 ng/m⁻³). Mercury concentrations did not vary significantly during the 24-h survey measurement, reporting an average value of 40.3 ± 0.75 ng/m³ (40.1 ng/m³ averages) and an extreme value of 235 ng/m³. In order to identify the possible TGM fate, a set of trajectories was obtained for different time periods using the wind fields from the Water Research and Forecasting (WRF) meteorological model and a dispersion was performed by using the CALPUFF model driven by the WRF-CALMET model to identify the TGM levels in the site vicinity.

Keywords Gaseous elemental mercury · San Joaquín · WFR model · Mercury dispersion · Mercury extraction

Introduction

The presence of mercury in the environment is mainly due to anthropogenic and natural sources; in addition, its study is very complex due to its different chemical forms. The mercury emission evaluation into the atmosphere raises serious methodological problems, which makes it difficult to differentiate between its origin from anthropogenic and natural emissions, and re-emissions from the soil or from marine aerosols (González-Carrasco et al. 2011). The mercury chemical species migration pathways can range from soil to atmosphere, water to soil, soil to plant, plant to atmosphere, and water to atmosphere, among others. These daily cycles of mercury emissions from soils, waters, or plants contribute to the increase of the atmospheric mercury reserve, especially in the lower layers of the troposphere. The total gaseous mercury (TGM) accounts for the gaseous elemental mercury (Hg⁰—GEM) and gaseous oxidized mercury (Hg²⁺—GOM) that are emitted by the anthropogenic and natural mercury sources into the atmosphere. On the other hand, a fraction of this mercury in its gaseous phase binds

✉ Rocío García-Martínez
gmrocio@atmosfera.unam.mx

¹ Centro de Ciencias de la Atmósfera, Universidad Nacional Autónoma de México, Ciudad Universitaria, 04510 Mexico, Mexico

² Centro de Geociencias, Universidad Nacional Autónoma de México, Campus Juriquilla, Bulevar. Juriquilla 3001, Querétaro 76230, México

³ Instituto de Geografía, Universidad Nacional Autónoma de México, Ciudad Universitaria, 04510 Mexico, Mexico

⁴ Instituto de Ingeniería, Universidad Nacional Autónoma de México, Ciudad Universitaria, 04510 Mexico, Mexico

⁵ Departamento de Geología, Universidad de Sonora, Rosales y Encinas, 83000 Hermosillo, Sonora, Mexico

⁶ Instituto Nacional de Ecología y Cambio Climático, 04530 Mexico City, Mexico

to particulate matter (PM) (Fu et al. 2012). GEM is the most abundant form of mercury in the atmosphere (95%) (GOM and PM are deposited quickly), due to its stability, volatility, and low solubility and its residence time ranging from approximately 0.5 to 2 years (Kabata-Pendias and Pendias 2001; Lindberg et al. 2007; Wan et al. 2009). The presence of toxic heavy metals such as arsenic (As), cadmium (Cd), mercury (Hg), and lead (Pb), in terms of concentration in the air, is low and well identified. Mercury has been considered a global pollutant due to its ability to migrate between different environmental compartments and its movement over long distances, resulting in the contamination of areas free from direct emission sources. The United States Government Agency for the Registration of Toxic Substances and Disease Registry has classified mercury as the third most toxic substance in the planet after arsenic and lead, due to its affectation at the cellular, cardiovascular, pulmonary, and renal levels; hematological; immunological; neurological; reproductive to name a few (Clifton, 2007; Rice et al. 2014). In Europe, diseases due to inhalation and/or exposure to mercury have decreased, due to recent control measures. However, adverse effects have been observed even with permissible exposure levels. In Slovenia, Hg is used for the manufacture of chlorine products, although its use was banned in December 2017. The use of coal for commercial, institutional, and domestic heating was responsible for 12% of mercury emissions in 2017, which occurred predominantly in central and Eastern Europe (Gworek et al. 2017). Currently, the mercury emission source with the greatest impact is the use of coal, which represents more than 50% of total anthropogenic emissions (UNEP, 2019), the burning of fossil fuels, and small-scale artisanal mining. The European Environment Agency (EEA 2017) considers that air pollution is a complex problem and multiple challenges are posed in terms of the management and mitigation of toxic and harmful pollutants. Previous studies have shown that the mercury contamination of the atmospheric air includes episodes of sudden drops in TGM concentrations in the Antarctic and Arctic (Schroeder et al. 1998). These interesting phenomena are called MDEs (mercury depletion events). This phenomenon is caused by the oxidation of GEM to its GOM form. GEM is characterized by a low value of Henry's law constant, which indicates its very low solubility in water (Skov et al. 2008; Seigneur et al. 1994; Rayaboshapko and Korolev 1997). This results in its long residence time in the air—even up to a year. However, in Antarctic conditions, its residence time is estimated to be only 10 h (Goodsite et al. 2004; Skov et al. 2004). Mercury events and ozone depletion during spring can also be observed in Antarctica, where they occur from late August to late October (Ebinghaus et al. 2002; Brooks et al. 2008; Witherow and Lyons 2008). The results showed that, as a result of its exhaustion in the air (spring, high radiation), the TGM fell from the “normal”

level of 1.1–1.2 to 0.9 ng/m³, with the minimum value of 0.1 ng/m³ (Ebinghaus et al., 2002). Pfaffhuber et al. (2012) obtained results in the GEM concentration of 1.0 ng/m³, while in the period of depletion of mercury in spring, it was 0.6 ng/m³, thus observing that when the vertical wind shear changes (Zhu et al. 2015; Fu et al. 2016; Zhu et al. 2016), thermodynamic stability (Llanos et al. 2011; Gustin et al. 2013), and water vapor content (Fu et al. 2016; Zhang et al. 2015; Zhu et al. 2016), TGM transport. High levels of GEM were detected over Antarctica during the day, representing 45% of global emissions; emissions of natural origin and re-emissions were estimated between 45 and 66% worldwide (Guan et al. 2010; UNE, 2019). Background condition studies carried out by Higuera et al. (2013; 2014) concluded that the most important factors that control emission, transport, and deposition processes are due to the temporal evolution of emissions in both daily and seasonal processes. The models used to evaluate the dispersion of mercury between the areas that represent the emission sources and the receiving areas have limited precision due to the lack of information and the null emission inventory at a global level in order to reduce the uncertainty level in their application (Pirrone et al. 2010). The current anthropogenic emissions of mercury contribute to future concentrations in the atmosphere; this element volatility favors its transport in the atmospheric circulation with a residence time in the air of approximately 0.5 years (Weiss-Penzias et al. 2003; 2015). The information available on this topic has been studied on a kilometer scale; unfortunately, information on the dispersion of TGM on a metric scale is scarce. It is difficult to estimate the amounts of mercury which end up in the atmosphere as a result of re-emission. China, Brazil, Indonesia, Colombia, Bolivia, Venezuela, and the Philippines emit much larger amounts of mercury from these sources, while the emissions from other countries are much less significant (Gworek et al. 2017). More than half of the mercury used for these purposes is consumed in South-East and South Asia and one-fourth of it in South America (Pacyna et al. 2008). The objectives of this study were to identify the TGM levels and evaluate its dispersion from mining sites in San Joaquín, Sierra Gorda Queretana (SGQ), a rural area located to 135 km northeast from Mexico City at an average height of 2440 amsl. In Mexico, the use of fossil fuels is being encouraged and the demand for elemental mercury is expected to continue, leading emissions in the upward trend in the upcoming years.

Materials and methods

Study area and sampling site

SGQ is part of the geological province of the Sierra Madre Oriental (SMO) in Mexico; it is formed by several deformed

and folded Mesozoic marine structures. To the south of the SGQ, there are important cinnabar (HgS) deposits along the great Mesoamerican territory. Cinnabar underground mining in the SGQ has a long history for the Mexican region; it has been dated to at least since 100 B.C. The San Joaquín region is located south of the SGQ, it has a population of 8865 inhabitants according to the last 2013 population census carried out by the National Institute of Statistics and Geography (INEGI, <http://www.inegi.org.mx>), in an area of approximately 212 km² where the mercury deposits can be found. It is located between 20° 51' 36" and 21° 03' 33" north latitude and between 99° 27' 28" and 99° 38' 25" west longitude, in the center-northeast of the state. It borders northwest with the municipality of Pinal de Amoles, to the north with Jalpan de Serra, and to the west and south with Cadereyta, which belongs to the Moctezuma river basin, approximately 92 and 134 km away from Querétaro City and Mexico City, respectively (De la Rosa et al. 2006). The SGQ has two mountainous ranges, the first with heights ranging from 2600 to 2620

amsl, the second, the central terrace where the historic city center is located, with contour lines between 2520 and 2560 amsl, is considered the lower part: it is a plain that rises a few meters, surrounded by a ridge of low, broken hills (Figs. 1 and 2). It has a varied climate; 51% of the surface has a dry and semi-dry climate in the central region; 24.3% has a warm subhumid climate in the SMO; 23% present temperate subhumid in the south and northeast; 1% has a warm humid climate towards the northeast; and the remaining 0.7% has a temperate humid climate in the northeast of the state. The annual average temperature is 18 °C; the average maximum temperature is 28 °C and occurs during April and May; the average minimum temperature is 6 °C during winter in January. Average rainfall is 570 mm per year; the state's rainy season runs from March to November, whereas the dry season runs from December to February.

The objective of this study was to evaluate both the dispersion and levels of TGM downwind of mercury mining areas located in San Joaquín, a rural area located in the



Fig. 1 Location of the San Joaquín (SJ) region. Information from the Statistical Framework INEGI, 2013



Fig. 2 View of the San Joaquin (SJ) region

Sierra Gorda Queretana (SGQ), 135 km northeast from Mexico City. The sampling site was selected following the National Atmospheric Deposition Program (NADP) guidelines. This protocol takes into account the orography of the study area the monitoring site consisted of a tailored monitoring shelter which was located in the geographic coordinates: $20^{\circ} 54' 41''$ N and $99^{\circ} 34' 13''$ W at an elevation of 2488 amsl, at around 2 km downwind of the mercury (Hg) emission sources (Fig. 3a and b). The TGM monitoring was carried out between March, April, and May 2015. A Tekran® model 2537A automatic mercury vapor analyzer was installed inside and operated following the protocols of the Global Mercury Observation System (GMOS) network (<http://www.gmos.eu/download/gmos-sop-tgm-gem>). The instrument measures the gaseous elemental mercury by passing the filtered sample air stream through two gold cartridges operating in parallel where it is trapped and thermally desorbed using ultra-high purity argon as the carrier gas following two operating modes (sampling and desorbing), and then detected using an integrated cold vapor atomic fluorescence spectrophotometer (CVAFS) detector

under a predetermined time of cycle (Tekran Instruments Corporation, 1999; Method IO-5 Sampling and Analysis of Vapor Mercury in Ambient Air Utilizing (US-Environmental Protection Agency-USEPA, 2003). The analyzer was programmed to measure an air sampling flow of 1.5 L/min. The sampling probe was held at an approximate height of 10 m above surface. The analyzer was configured to perform an automatic calibration every 24 h with the internal permeation tube procedure using zero air provided by a Tekran® model 1100 zero air. Average TGM concentrations were obtained every 5 min/h during 24 h. Measurements were followed online in order to determine spatial variation and operating problems. The results were evaluated weekly and monthly throughout the sampling period. According to the manufacturer, the detection limit of the instrument is 0.1 ng/m^3 Hg, with a measurement error of less than 2% (ASTM D-6784-02, 2002; CFR 40, Part 60 2005). Tekran® analyzers have been widely used to measure TGM during the last 15 years (Landis et al. 2002).

The WRF v3.8.1 meteorological data used for modeling with the WRF program is a weather data from the National

Fig. 3 **a** Tekran® model 2537A automatic mercury vapor analyzer and **b** measurement station



Climatic Data Center (NCDC) and the National Oceanic and Atmospheric Administration (NOAA). The WRF was used with the following parameterizations MP_PHYSICS = 4, RA_LW_PHYSICS = 1, RA_SW_PHYSICS = 2, SF_SFCLAY_PHYSICS = 1, SF_SURFACE_PHYSICS = 2, BL_PBL_PHYSICS = 1, and CU_PHYSICS = 5. The downloaded final analysis files are of type GRIB2, in cells of 0.25×0.25 , that is, cells of approximately $25 \text{ km} \times 25 \text{ km}$. Mercury dispersion was estimated to identify emission sources and the WRF, CALWRF v1.1, CALMET v6, and CALPUFF v6 were used to assess mercury dispersion to nearby regions. The WRF is a non-hydrostatic numerical mesoscale weather forecast system, developed to be applied in a prognosis mode for the study of meteorological phenomena. CALWRF was used to process WRF output to be used by CALMET. CALPUFF is a model of the United States Environmental Protection Agency (USEPA 2003); it requires two separate calculation modules: CALMET to analyze and define meteorological variables, and CALPUFF to simulate the dispersion of pollutants. CALPUFF simulates air pollutant emissions from a given source as a series of “puffs.”

Mercury regulation in Mexico

In Mexico, there is no regulation regarding values emitted and/or present in ambient air for mercury or its compounds. However, as a guide value, the maximum permitted values, proposed by the California Air Resources Board in its *Consolidated Table of OEHHA/ARB Approved Risk Assessment Health Values* (OEHHA/ARB, 2019), will be considered. The corresponding reference exposure levels for mercury and its inorganic compounds are shown in Table 1. The presented values were revised or imposed in December 2008 and corresponded to maximum values associated with effects other than cancer.

Results and discussion

Measured mercury concentrations

The extraction of Hg is as follows:

Table 1 Applicable regulations; reference values for human exposure to mercury and its compounds (OEHHA/ARB, 2019)

Type of exposure	Limit value (ng/m ³)
Acute inhalation	600
Inhalation during 8 h	60
Chronic inhalation	30

- i) The furnaces used for the extraction of Hg consist of a series of iron tubes 8" to 12" in diameter (Fig. 4a), connected to a red brick artisanal heating chamber (Fig. 4b),
- ii) The cinnabar is placed inside each tube connected, and closed with a steel lid that is sealed with mud (Fig. 4c), and the kilns work with direct heating; opposite sides of the steel lid are tubes of smaller diameter,
- iii) The tubes flow into a mud container called a condensation chamber where the mercury vapor is trapped and condensed,
- iv) The maximum cinnabar load that a furnace supports with these characteristics is 200 kg (Fig. 5).

The data analysis was carried out in a Microsoft Excel database; a statistical software SPSS for Windows version 12 was used. Methods and control mechanisms designed to guarantee the quality of the data in all stages of the investigation were implemented. The data were worked by applying descriptive statistics to obtain measures of central tendency and dispersion, in the case of the mean numerical variables, and for the categorical variable percentages. To guarantee the quality of the data and identify outliers, the statistical technique (outliers) that worked with quartiles and interquartile was used for the entire data set (Yang et al. 2005; Chandler and Scott 2011). Table 2 shows the number of data, and the average, median, minimum, maximum, 25th and 75th percentiles, and standard deviation corresponding to the sampling period from March to May; the values obtained emphasize the variability of TGM concentrations. The mean mercury concentration for a 24-h period takes these fluctuations into account and is considered representative of the impact of mining activity in the area. The minimum period to see a trend is 24 h, since the mercury concentration depends on the temperature.

The hourly averaged TGM concentrations were obtained every 5 min during 24 corresponding to the months of March, April, and May 2015 (Fig. 6a–c, respectively). The values observed are in a range of 40 to 41 ng/m³, above the chronic concentration value of 30 ng/m³, and the maximum concentrations obtained were in the range 184 to 235 ng/m³ during the period of sampling. Concentrations were obtained for a period of 8 h obtaining values in the range of 67 and 74 ng/m³, observing concentration values greater than 60 ng m⁻³ according to the recommendations of the Air Resources Board of California in its *Consolidated Table of OEHHA/ARB Approved Risk Assessment Health Values* (OEHHA/ARB, 2019). The results obtained agree with that reported by Hernández-Silva et al. (2012) in the same region where a value of 67 ng/m³ and a maximum value of 416.0 ng/m³. When observing the results obtained at Sisal, Yucatán, in 2013, the concentrations were in a range of 0.5 to 3.9 ng/m³ with an annual average concentration of $1163 \pm 0.250 \text{ ng/m}^3$.

Fig. 4 **a** Furnaces used for the extraction of Hg consist of a series of iron tubes 8" to 12" in diameter. **b** Brick artisanal heating chamber. **c** Condensation tubes and mercury vapor chamber

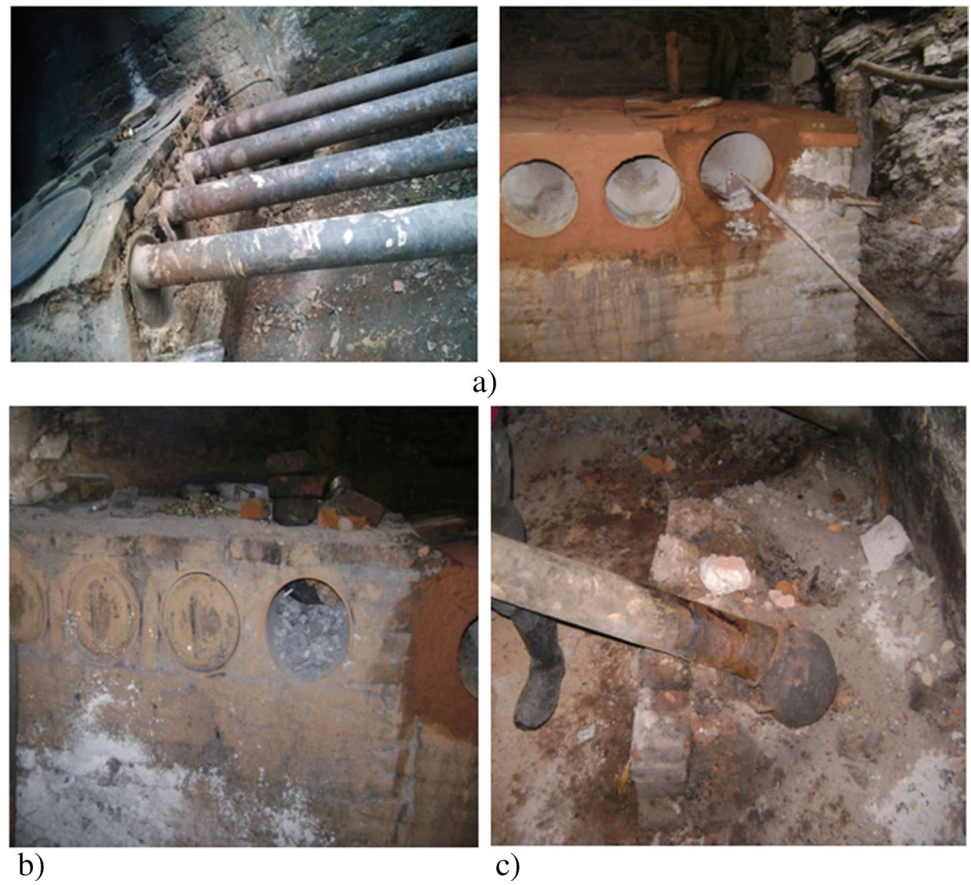


Fig. 5 Location of the mining deposits registered (Council of Mineral Resources, 2014) State of Querétaro, Mexico

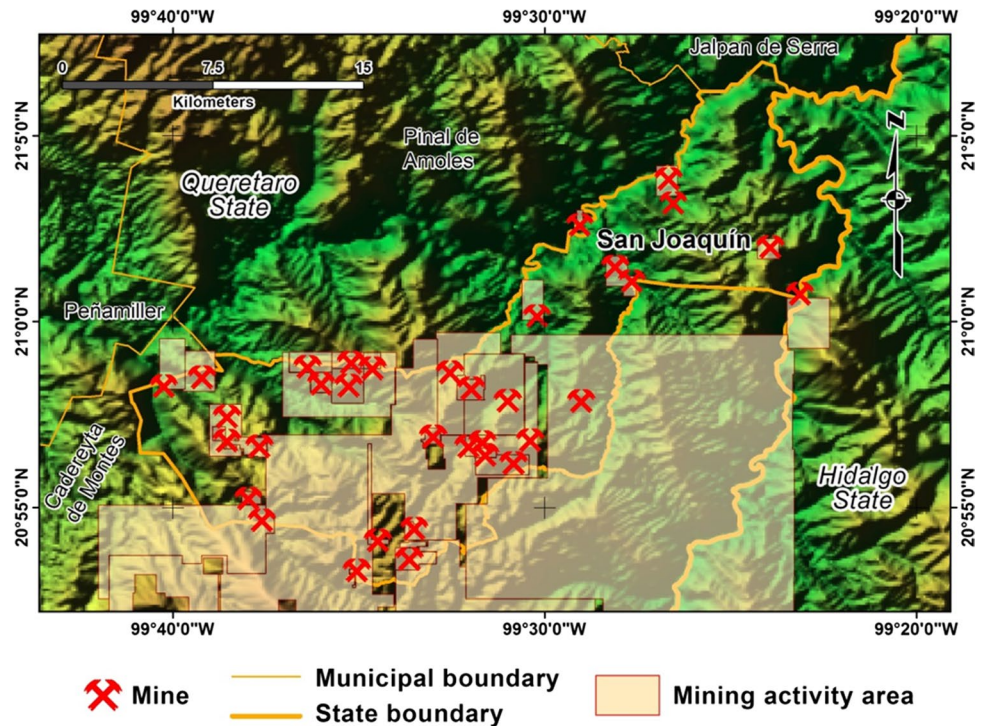


Table 2 Descriptive statistics: average, median, minimum (Min), maximum (Max), 25th and 75th percentiles, standard deviation (Std. Dev.), and number of determination (*N*) concentrations of TGM (ng/m³) at San Joaquín, Qro., for March, April, and May 2015 (Fig. 6a–c), respectively

Hg (ng/m ³)	Average	Median	Min	Max	25th percentile	75th percentile	Std. Dev	<i>N</i>
March	41.20	36.7	0.894	183.75	20.25	123.60	2.19	5317
April	39.9	37.1	0.21	235.0	18.33	119.7	1.22	8431
May	6.1	4.5	0.1	133.6	3.53	18.21	0.32	8826

m³. Our study shows evidence of an environmental exposure of TGM, originated not only from the Hg extraction process, but also from the sites where the ore is processed. In addition, mercury levels vary considerably according to the location and type of mining process.

On the other hand, the average concentrations of mercury in the air reported in the present study are above those registered in this site and other rural areas such as Puerto Ángel (coast of Oaxaca, along the Pacific, in southeastern Mexico) and Huejutla (rural area in the state of Hidalgo, in eastern Mexico), where average values of 1.46 and 1.32 ng/m³ were determined, respectively (De la Rosa et al. 2004). The results obtained are consistent with those reported by Higuera et al. (2013, 2014) and Isbrí et al. (2020). A moving average of 1 and 12 h was applied to the results obtained to soften the curves and eliminate variations. Isbrí et al. (2020) reported the results obtained from TGM horizontally and vertically in the dispersion of TGM derived from a mining source, showing clear differences between “classic” seasons and “transition” seasons in terms of limits between normal and anomalous populations. In this sense, in summer and winter, there is a break between normal and transitional populations at similar levels (6.76 ng/m³ in winter and 7.73 ng/m³ in summer), while in spring, this break occurs at higher levels (14.81 to 275 ng/m³), and during autumn, it occurs at 10.36 ng/m³. In profile 1, the anomalous population corresponds to the emissions of Azogues riverbank sediment and these are detectable at mercury levels of 10 ng/m³ in drier seasons (autumn and summer) and up to 30.14 ng/m³ in wet seasons (winter and spring); it should be remembered that this profile does not have any significant emission sources, except for polluted sediments, and the background values are below 10–14 ng/m³ in all seasons. Once we had identified the micrometeorological conditions in which there was a risk, we proceeded to identify the extent of this risk in space. In the time series (Fig. 6a–c) of the concentrations for March–April–May 2015, it can be seen that there is no defined weekly or daily trend in any of the three sampled months of 2015, taking into account that the average concentration in March and April is in a range of 40 to 41 ng/m³, unlike the month of May, when concentration is approximately seven times smaller: this is probably due to the pronounced rainy season in the region. Likewise, the dispersion of the data during the three months is large, which may be

due to factors such as instrumentation, environmental conditions, or mining activity that reflects irregular behavior.

Mercury emission trajectories

Forward trajectories using WRF wind fields are presented, to characterize the possible paths from the monitoring site and possible fate of the emissions during 8-h time length. The mercury emission area of influence in the San Joaquín region was identified, with two modeling domains: one covering most of the country (domain a), and another, with higher resolution, used to observe the regional impact of possible trajectories of mercury emissions (domain b). Figure 7a shows the major domain modeling area, which has 15-km cells. Figure 7b shows the modeling domain of the minor domain, which includes 5-km cells.

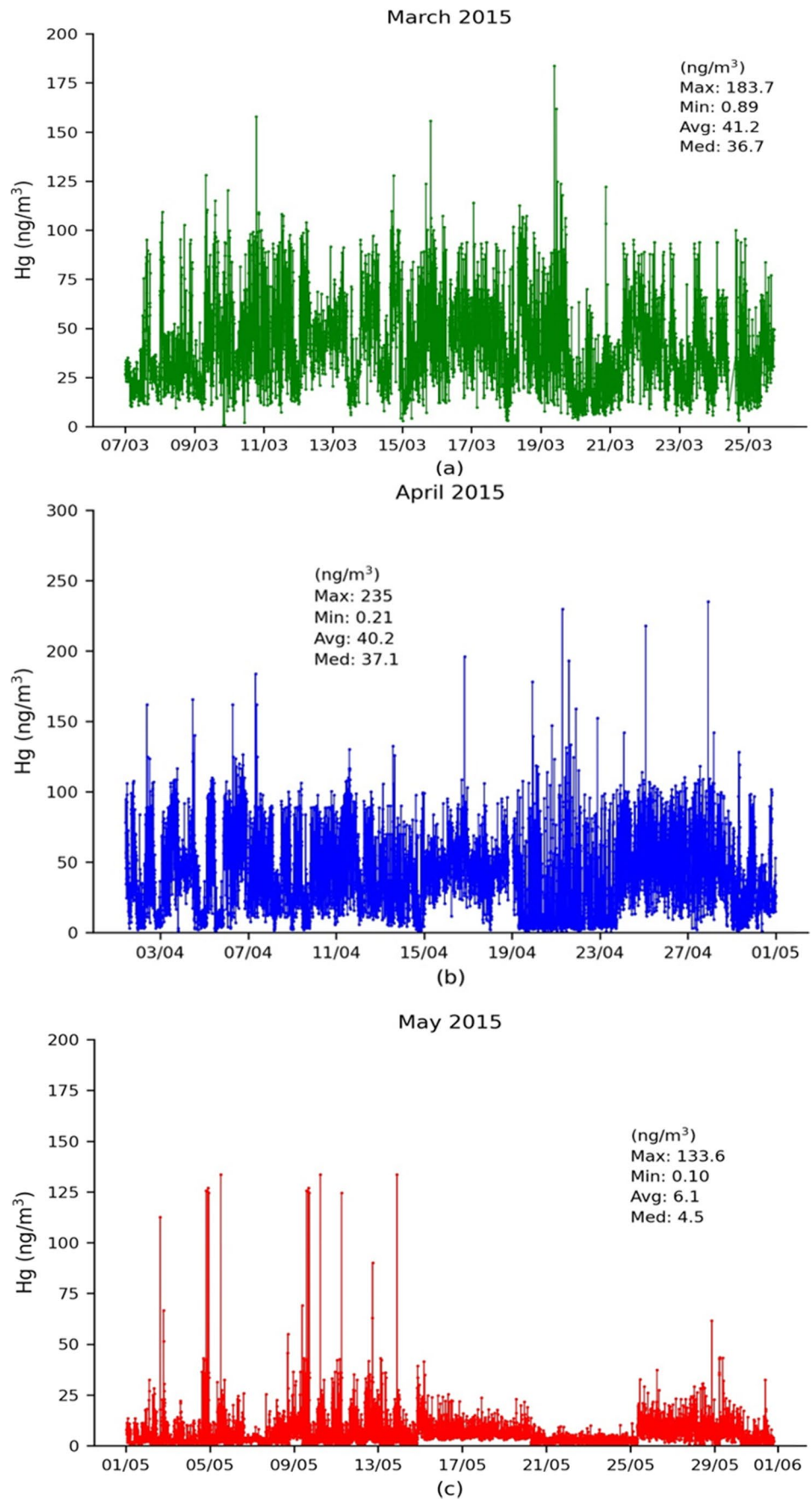
Domain b was used for the estimation of the trajectories: in the trajectory modeling of March and April from 2015, it is observed that the area of influence of mercury dispersion is towards the cities of San Joaquin (SJq), Querétaro (Qro), Celaya (Cel), San Luis Potosí (SLP), Morelos (Mor), and Metropolitan Area of the Valley of Mexico (ZMVM, for its initials in Spanish) as shown in Fig. 8.

The meteorological information used to run the WRF comes from final analysis (NCEP FNL 2015). Nineteen days that are representative of the meteorology of 2012 were considered to make an estimate of the possible regions of influence of emissions. Subsequently, 12 of those 19 episodes, the ones that have influence on urban areas, were selected to carry out a modeling of dispersion of emissions using the CALPUFF model: the twelve dates considered are January 13, February 8, March 21, April 17, May 14, June 10, July 20, August 30, September 12, October 9, November 16, and December 17. Four dates with trajectories that reach Querétaro City were selected (Fig. 9).

Local influence the mining site

As result of the modeling with CALPUFF atmospheric dispersion model, for the period from March 7 to 25, 2015, the concentration of Hg was calculated for the San Joaquín region, where the Tekran mercury analyzer was located in order to compare the model with the measured records. These results are shown in Figs. 10 and 11, where the color

Fig. 6 a, b, and c TGM were obtained every 5 min during 24 (March, April and May 2015)



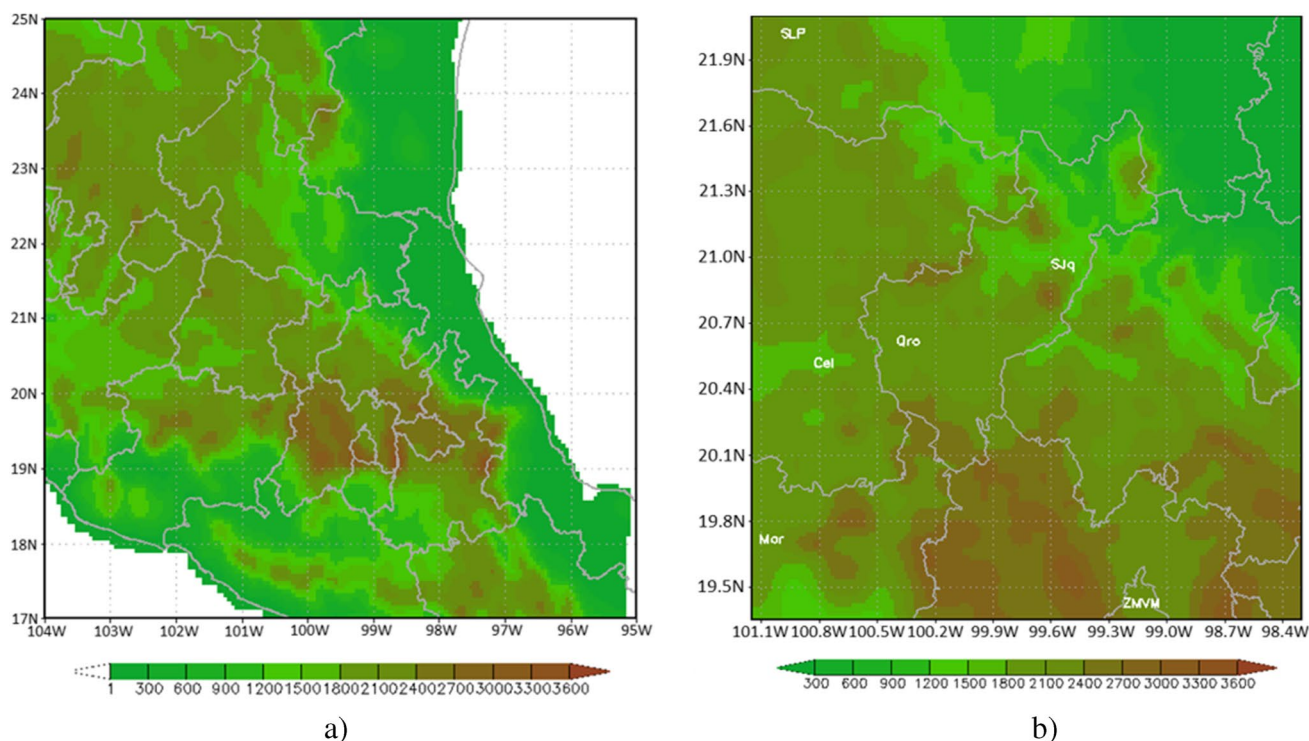


Fig. 7 Modeling area of the major domain (a) and internal domain (b) for emission paths; the topography and the political division are shown. San Joaquín (SJq), Querétaro (Qro), Celaya (Cel), San Luis

Potosí (SLP), Morelos (Mor), and Metropolitan Area of the Valley of Mexico (ZMVM)

scale corresponds to the limit values presented in Table 1. The blue value corresponds to the limit for chronic inhalation and can be used to compare the average concentration of 24 h; green corresponds to the limit for inhalation for 8 h; yellow corresponds to an approximate limit value for 1 h; and finally, red corresponds to the value that should not exceed in order to prevent acute inhalation. Four dates of trajectories traced by the CALPUFF model were randomly selected and plotted in Fig. 11, where the maximum hourly concentrations of atmospheric Hg estimated are also shown. It is observed that Hg generated in the mining area might reach Querétaro in the previously mentioned days. It is also observed that mercury contamination is local, and that the entire mining area generally has mercury concentration values above the average 8-h threshold value.

Similar conclusions are reached for the period March–April 2015, than for previous periods: the population affected by the presence of mercury in the vicinity of mines and/or furnace areas is significant, as concentrations exceed the suggested limit value for acute exposure (600 ng/m^3). Likewise, the emissions generated in San Joaquín can reach Querétaro depending on the prevailing weather conditions. Hourly average values between 10 and 30 ng/m^3 can be observed (only hourly data in March and April 2015

above 10 ng/m^3); however, the daily average values are well below 30 ng/m^3 , thus modeling with CALPUFF suggests that chronic effects by Hg in the population of Querétaro are not expected as a direct effect of the emissions from the San Joaquín mining area, at current production levels. The above is shown in Fig. 11a and b, which show the maximum hourly mercury concentrations for March and April 2015, respectively.

Conclusions

Our work shown here concludes two important aspects to consider: First, the dispersion of TGM is extensive and permanent. This is a consequence of the fact that the Sierra Gorda Queretana (SGQ) and in particular the San Joaquín (SJ) region have almost 60% of the mines that operate with open-pit artisanal furnaces in the region. Second, the average TGM levels measured in the air significantly exceeded the Agency for Toxic Substances and Disease Registry minimum hazard level of 200 ng/m^3 (ATSDR 2010); therefore, a potential risk for the exposed population can be considered, since according to WHO-IPCS31, the levels of mercury in the air for rural areas should be

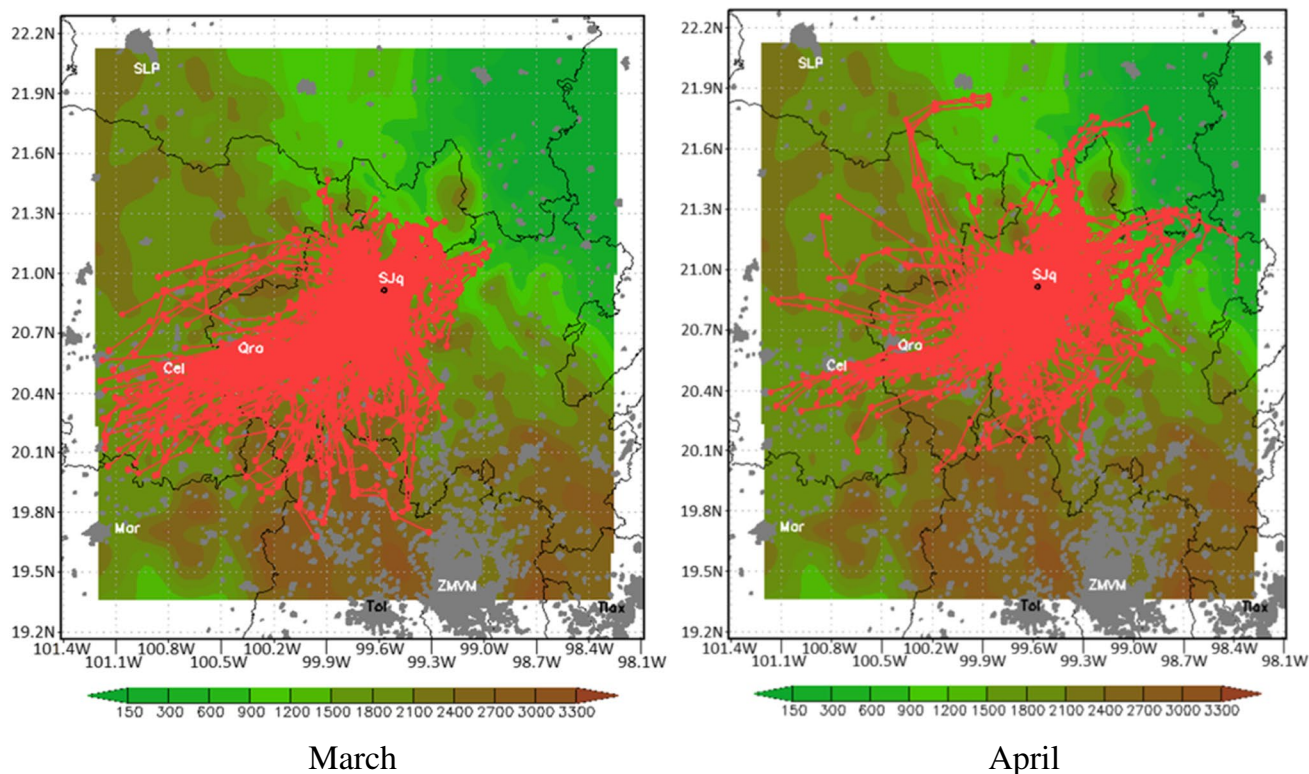


Fig. 8 Topography (green–brown), urban area (gray), and hourly trajectories (red) of San Joaquín emissions during March and April 2015. Each point represents 1 h; the route is 8 h from San Joaquín.

San Joaquín (SJq), Querétaro (Qro), Celaya (Cel), San Luis Potosí (SLP), Morelos (Mor), and Metropolitan Zone of the Valley of Mexico (ZMVM)

in a range of 2 to 4 ng/m^3 and around 10 ng/m^3 in urban areas. In addition to the release of TGM, the San Joaquín region is suffering other environmental impacts; with the use of the models, it was possible to observe long-range transport and a large discrepancy in altitudes below 1.5 km due to the mountainous landscape that exists in the region, observed with the results from the models used. From the dispersion modeling meteorology, it can be observed in the analysis of trajectories that emissions can be transported towards multiple directions: in the east, arriving in the city of Querétaro and continuing to Celaya, in some cases traveling southeast and reaching Morelia, other times they travel to the north and reach San Luis Potosí, or they can

be transported to the south and thereby arrive to the north of the Metropolitan Area of the Valley of Mexico. Previous work supports these findings and offer more concrete evidence on the magnitudes and importance of dispersion related to mercury from mining regions (Higuera et al. 2006, 2013, 2014; Pirrone et al. 2010; Esbrí et al. 2020). According to the results obtained, the authors recommend that future studies consider more sites to measure the large-scale transport in the prediction models. In addition, aerosol data, such as MODIS data and the vertical profile, can be used to verify the spatial distribution of mercury atmospheric and provide a more robust comparison of the vertical mercury vapor and temperature profiles.

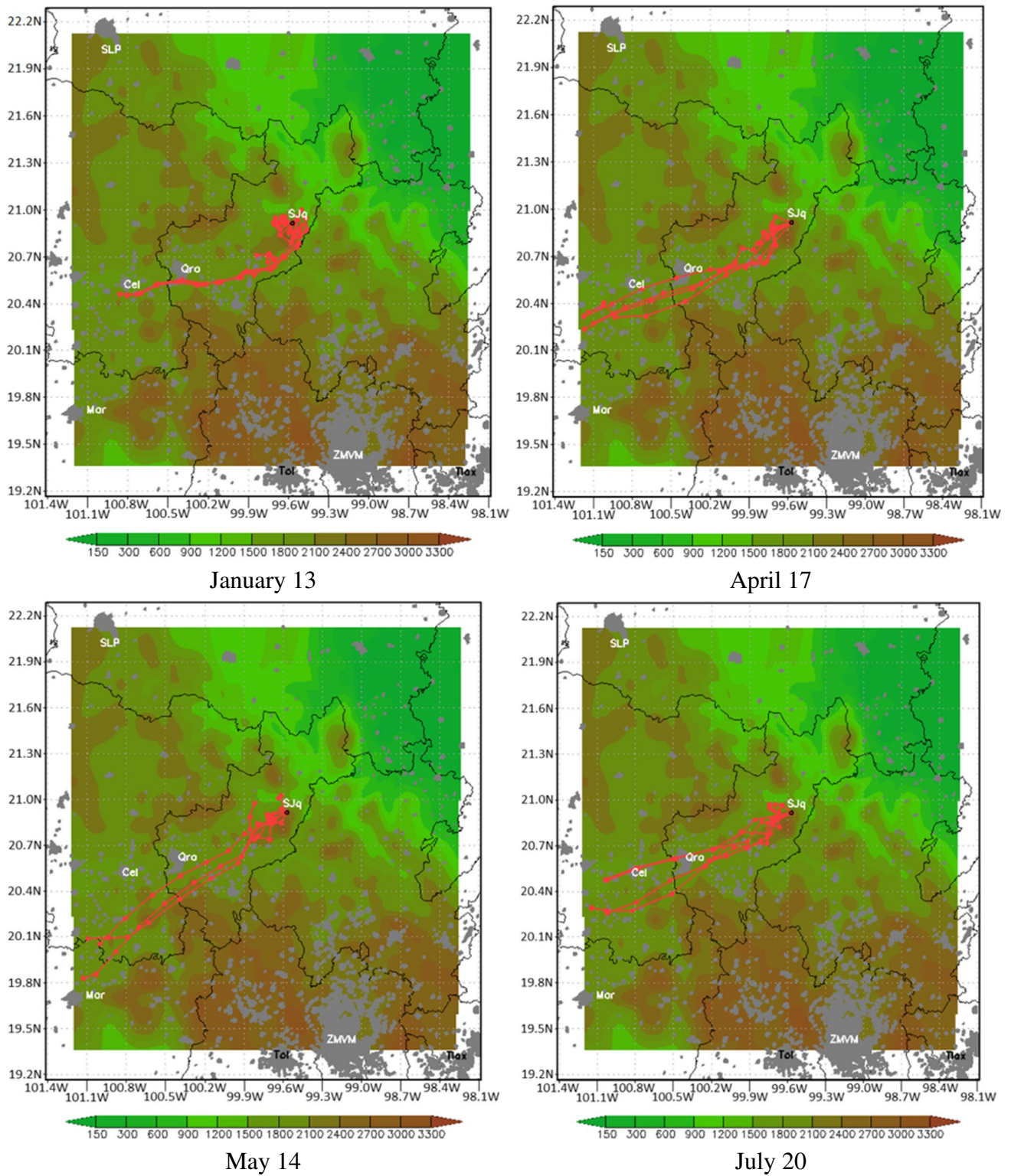


Fig. 9 Trajectories calculated for the selected month and days corresponding to January 13, April 17, May 14, and July 20, 2012. San Joaquín (SJq), Querétaro (Qro), Celaya (Cel), San Luis Potosí (SLP), Morelos (Mor), and Metropolitan Area of the Valley of Mexico (ZMVM)

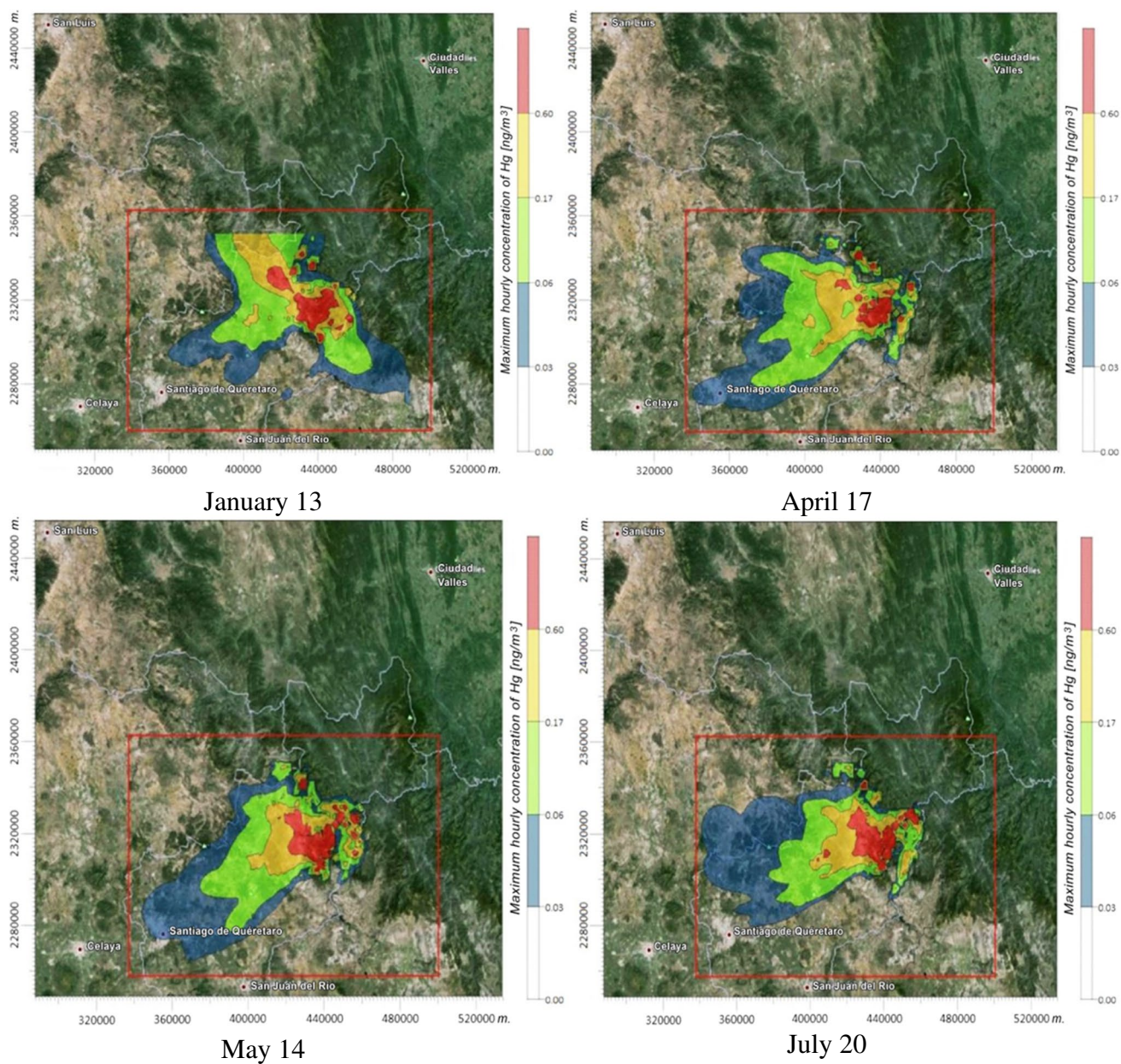


Fig. 10 Maximum hourly concentrations of Hg corresponding to January 13, April 17, May 14, and July 20, 2012. CALPUFF atmospheric dispersion model

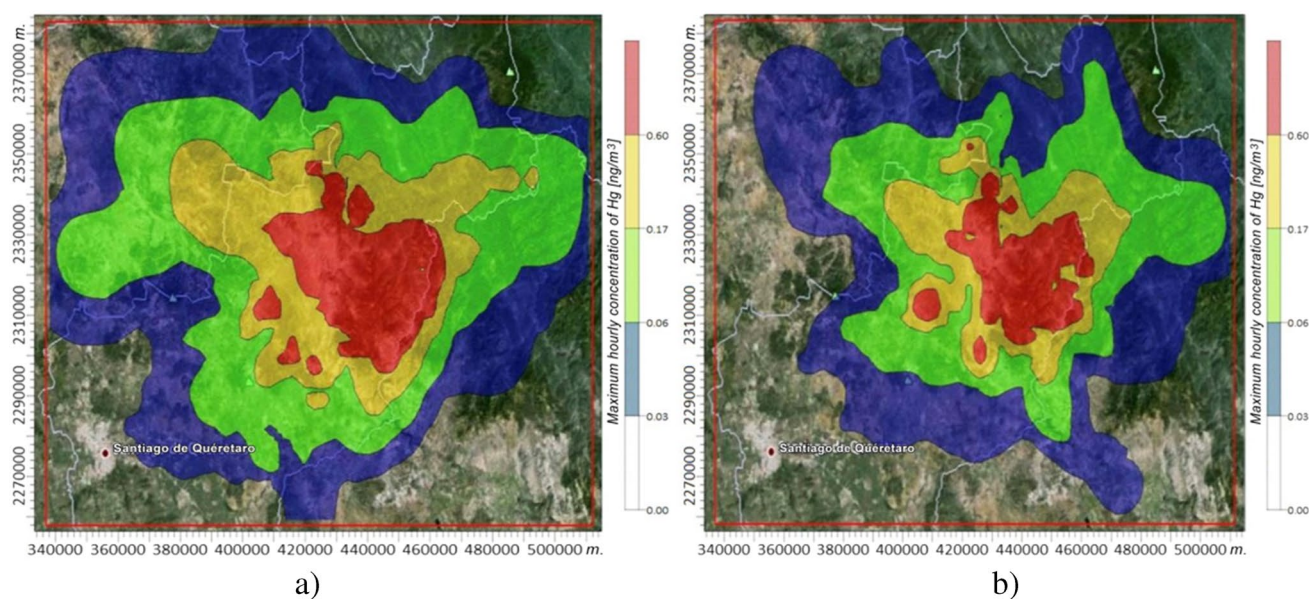


Fig. 11 Maximum hourly concentration of atmospheric mercury from March 2 to March 21, 2015 (a) and April 16 to April 29, 2015 (b). CAL-PUFF atmospheric dispersion model

Acknowledgements We thank Manuel Garcia and Wilfrido Gutiérrez for their technical support and Martin Rangel, Isela Martinez, and Moises Lopez of Postgraduate Program at the National Autonomous University of México (UNAM for its initials in Spanish).

Funding This work was funded by grant National Institute of Ecology and Climate Change, México (INECC for its initials in Spanish).

Data availability Raw data is not publicly available; data requests can be made to the corresponding author: PhD. Rocío García through this email: “gmrocio@atmosfera.unam.mx”.

Code availability The code is available from the corresponding author by request.

References

- ASTM- Standard test method for elemental, oxidized, particle-bound and total mercury in flue gas generated from coal-fired stationary sources (Ontario Hydro Method), ASTM D-6784-02, 2002; CFR 40, Part 60, 2005 (2002) American Society for Testing and Materials, West Conshohocken, PA
- ATSDR- Agency for Toxic Substances and Disease Registry (2010) Minimal risk levels (MRLs) for hazardous substances. Agency for Toxic Substances and Disease Registry. <http://www.atsdr.cdc.gov/mrls/mrllist.asp>.
- Brooks S, Lindberg S, Southworth G, Arimoto R (2008) Springtime atmospheric mercury speciation in the McMurdo Antarctica Coastal Region. *Atmos Environ* 42(12):2885–2893. <https://doi.org/10.1016/j.atmosenv.2007.06.038>
- Clifton JC (2007) 2nd. Mercury exposure and public health. *Pediatric Clinic North America* 54(2):237-viii. <https://doi.org/10.1016/j.pcl.2007.02>
- De la Rosa DA, Velasco A, Rosas A, Volke-Sepúlveda T (2006) Total gaseous mercury and volatile organic compounds measurements at five municipal solid waste disposal sites surrounding the Mexico City Metropolitan Area. *Atmos Environ* 40:2079–2088. <https://doi.org/10.1016/j.atmosenv.2005>
- De la Rosa T, Volke-Sepúlveda G, Solórzano C, Green R, Tordon SB (2004) Survey of atmospheric total gaseous mercury in Mexico. *Atmos Environ* 38(29):4839–4846. <https://doi.org/10.1016/j.atmosenv.2004.06>
- Ebinghaus R, Kock HH, Temme C et al (2002) Antarctic spring-time depletion of atmospheric mercury. *Environ Sci Technol* 36(6):1238–1244
- European Environment Agency (EEA) (2017) Air Quality in Europe report. <https://doi.org/10.2800/850018>
- Esbrí JM, Higuera PL, Martínez-Coronado A, Naharro R. 4D dispersion of total gaseous mercury derived from a mining source: identification of criteria to assess risks related with high concentrations of atmospheric mercury. *AtmosChemPhys Discuss*. <https://doi.org/10.5194/acp-2019-1107>
- Fu XW, Feng X, Shang LH, Wang SF, Zhang H (2012) Two years of measurements of atmospheric total gaseous mercury (TGM) at a remote site in Mt. Changbai area, Northeastern China. *Atmos Chem Phys* 12:4215–4226. <https://doi.org/10.5194/acp-12-4215>
- Fu XW, Zhu W, Zhang H, Wang X, Sommar J, Yang X, Lin CJ, Feng XB (2016) Depletion of atmospheric gaseous elemental mercury by plant uptake at Mt. Changbai, Northeast China. *Atmos Chem Phys* 16(20):12861–12873. <https://doi.org/10.5194/acp-16-12861-20>
- González-Carrasco V, Velasquez-Lopez PC, Olivero-Verbel J, Pájaro-Castro N (2011) Air mercury contamination in the gold mining town of Portovelo, Ecuador. *Bull Environ Contam Toxicol* 87(3):250–253. <https://doi.org/10.1007/s00128-011-0345-5>
- Goodsite ME, Plane JM, Skov H (2004) (2004) A theoretical study of the oxidation of Hg⁰ to HgBr₂ in the troposphere. *Environ Sci Technol*. 38(6):1772–1776. <https://doi.org/10.1021/es034680>
- Guan ZG, Lundin P, Somesfalean Mei L, G, Svanberg S. (2010) Vertical lidar sounding of atomic mercury and nitric oxide in a major

- Chinese city. *Appl Phys B*. 101:465–470. <https://doi.org/10.1007/s00340-010-4166-8>
- Gustin MS, Huang J, Miller MB, Peterson C, Jaffe DA, Ambrose J, Finley BD, Lyman SN, Call K, Talbot R, Feddersen D, Mao H, Lindberg SE (2013) Do we understand what the mercury speciation instruments are actually measuring? Results of RAMIX. *Environ Sci Technol* 47(13):7295–7306. <https://doi.org/10.1021/es3039104>
- Gworek B, Dmuchowski W, Baczewska, Baczewska AH, Bragoszewska P, Kalabun OB, Justyna WJ (2017) Air contamination by mercury, emissions and transformations a review. *Water Air Soil Pollut*. 228:123
- Higuera P, Oyarzun R, Lillo J, Sánchez-Hernández JC, Molina JA, Esbrí JM, Lorenzo S (2006) The Almadén district (Spain): 445 anatomy of one of the world's largest hg-contaminated sites. *Sci Total Environ* 356(1–3):112–124. <https://doi.org/10.1016/j.scitotenv.2005.04.042>
- Higuera P, María Esbrí, J., Oyarzun, R., Llanos, W., Martínez-Coronado, A., Lillo, J., López-Berdonces, M.A., García-Noguero, E. M (2013) Industrial and natural sources of gaseous elemental mercury in the Almadén district (Spain): an updated report on this issue after the ceasing of mining and metallurgical activities in 2003 and major land reclamation works. *Environmental Research* 125:197–208, 2013. <https://doi.org/10.1016/j.envres.2012.10.011> **Get rights and content**
- Higuera P, Oyarzun R, Kotnik J, Esbrí JM, Martínez-Coronado A, Horvat M, López-Berdonces MA, Llanos W, Vaselli O, Nisi B, Mashyanov N, Ryzov V, Spiric Z, Panichev N, McCrindle R, Feng X, Fu X, Lillo J, Loredó J, García ME, Alfonso P, Villegas K, Palacios S, Oyarzún J, Maturana H, Contreras F, Adams M, Ribeiro-Guevara S, Niecenski L F, Giammanco S, Huremovic J (2014) A compilation of field surveys on gaseous elemental mercury (GEM) from contrasting environmental settings in Europe, South America, South Africa and China: separating fads from facts *Environmental Geochemistry and Health* 36(4), 713–734. <http://hdl.handle.net/2117/24259>: <https://doi.org/10.1007/s10653-013-9591-2>. ISSN0269–4042
- Investigation of the light-enhanced emission of mercury from naturally enriched substrates *Atmospheric Environment* (R827622E02) American Chemical Society, Washington, DC, 36(20):3241–3254
- Kabata-Pendias A, Pendias H (2001) Trace elements in soils and plants, 3rd edn. CRC Press, Boca Raton, London, New York
- Lindberg S, Bullock R, Ebinghaus R, Engstrom D, Feng X, Fitzgerald W, Pirrone N, Prestbo E, Seigneur C. (2007). Panel on Source Attribution of Atmospheric Mercury. A synthesis of progress and uncertainties in attributing the sources of mercury in deposition. *Ambio*. <https://doi.org/10.1579/0044-744>
- Llanos W, Kocman D, Higuera P, Horvat M (2011) Mercury emission and dispersion models from soils contaminated by cinnabar 465 mining and metallurgy. *J Environ Monit* 13:3460–3468. <https://doi.org/10.1039/c1em10694>
- National Centers for Environmental Prediction/National Weather Service/NOAA/U.S. Department of Commerce (2015): NCEP GDAS/FNL 0.25 Degree Global Tropospheric Analyses and Forecast Grids. Research Data Archive at the National Center for Atmospheric Research, Computational and Information Systems Laboratory. Dataset. <https://doi.org/10.5065/D65Q4T4Z>
- OEHHA/ARB: Office of Environmental Health Hazard Assessment and Air Resources Board: Approved Risk Assessment Health Values; Sacramento, CA. (2019) www.arb.ca.gov/toxics/healthval/contable. The OEHHA has adopted three technical support documents for these guidelines, which can be found on their website: http://www.oehha.ca.gov/air/hot_spots/index.html
- Pfaffhuber KA, Berg T, Hirdman D, Stohl A (2012) Atmospheric mercury observations from Antarctica: seasonal variation and source and sink region calculations. *Atmospheric Chemistry and Physics* 12:3241–3251. <https://doi.org/10.5194/acp-12-3241-2012>
- Pacyna, J. M., Munthe, J., Wilson, S. (2008). Global emission of mercury to the atmosphere. In: AMAP/UNEP, technical background report to the global atmospheric mercury assessment Arctic Monitoring and Assessment Programme, UNEP Chemical Branch. *Atmospheric Environment* 44(20):2487–2499, <https://doi.org/10.1016/j.atmosenv.2009.06.009>
- Pirrone N, Cinnirella S, Feng X, Finkelman RB, Friedli HR, Leaner J, Mason R, Mukherjee AB, Stracher GB, Streets DG, Telmer K (2010) Global mercury emissions to the atmosphere from anthropogenic and natural sources. *Atmos Chem Phys* 10:5951–5964. <https://doi.org/10.5194/acp-10-5951-2010>
- Rayaboshapko, A. G., & Korolev, V. A. (1997). Mercury in the atmosphere: estimation of model parameters. Meteorological Synthesizing Centre - East, EMEP/MSC-E, Report 7/97, Moscow.
- Rice KM, Walker EM Jr, Wu M, Gillette C, Blough ER (2014) Environmental mercury and its toxic effects. *J Prev Med Public Health* 47(2):74–83. <https://doi.org/10.3961/jpmph.2014.47.2.74>
- Schroeder WH, Anlauf KG, Barrie LA, Lu JY, Steffen A, Schneeberger DR et al (1998) Arctic springtime depletion of mercury. *Nature* 394:331–332. <https://doi.org/10.1038/28530>
- Seigneur C, Wrobel J, Constantinou E (1994) A chemical kinetic mechanism for atmospheric inorganic mercury. *Environ Sci Technol*. 28(9):1589–9. <https://doi.org/10.1021/es00058a009>
- Skov H, Christensen JH, Goodsite ME, Heidam NZ, Jensen B, Wählin P, Geernaert G (2004) Fate of elemental mercury in the Arctic during atmospheric mercury depletion episodes and the load of atmospheric mercury to the Arctic. *Environmental Science Technology* 38(8):2373–2382. <https://doi.org/10.1021/es030080h>
- Skov, H., Bullock, R., Christensen, J. H., Sørensen, L. L (2008) Atmospheric pathways. In: AMAP/UNEP, technical background report to the global atmospheric mercury assessment. Arctic Monitoring and Assessment Programme/ UNEP Chemicals Branch, pp159.
- Statistical methods for trend detection and analysis in the environmental sciences. John Wiley and Sons Ltd., West Sussex, Reino Unido, 388
- Tekran Instruments Corporation (1999) Model 2537A Mercury Vapour Analyzer: User Manual. Ontario, Toronto
- UNEP- United Nations Environmental (2019) Global Mercury Assessment 2018. UN Environment Programme, Chemicals and Health Branch Geneva, Switzerland. ISBN: 978–92–807–3744–8.
- US-Environmental Protection Agency (2003) Support Center for Regulatory Atmospheric Modeling (SCRAM). Air Quality Dispersion Modeling - Alternative Models.
- Wan Q, Feng X, Lu J, Zheng W, Song X, Han S, Xu H (2009) Atmospheric mercury in Changbai Mountain area, northeastern China I. The seasonal distribution pattern of total gaseous mercury and its potential sources. *Environmental Research*. 109(3):201–206. <https://doi.org/10.1016/j.envres.2008w>
- Weiss-Penzias P, Jaffe AD, McClintick A, Prestbo EM, Landis M (2003) S (2003) Gaseous elemental mercury in the marine boundary layer: evidence for rapid removal in anthropogenic pollution. *Environ Sci Technol* 37(17):3755–3763. <https://doi.org/10.1021/es0341081>
- Weiss-Penzias P, Amos HM, Selin NE, Gustin MS, Jaffe DA, Obrist D, Sheu G-R, Giang A (2015) Use of a global model to understand speciated atmospheric mercury observations at five high-elevation sites. *Atmos Chem Phys* 15:1161–1173. <https://doi.org/10.5194/acp15-1161>
- Wetherow RA, Lyons WB. (2008). Mercury deposition in a polar desert ecosystem. *Environmental Science and Technology* 2008 42 (13), 4710–4716. <https://doi.org/10.1021/es800022g>
- Yang WY, Cao W, Chung T-S, y Morris J. (2005) Applied numerical methods using Matlab. John Wiley & Sons, Nueva Jersey, EUA, p 511

- Zhang L, Wang S, Wang L, Wu Y, Duan L, Wu O, Wang F, Yang M, Yang H, Hao J, Liu X (2015) Updated emission inventories for speciated atmospheric mercury from anthropogenic sources in China. *Environ Sci Technol* 49(5):3185–3194. <https://doi.org/10.1021/es504840m>
- Zhu W, Sommar J, Lin C-J, Feng X (2015) Mercury vapor air–surface exchange measured by collocated micrometeorological and enclosure methods – part I: data comparability and method characteristics. *Atmos Chem Phys* 15:685–702. <https://doi.org/10.5194/acp-15-685-2015>
- Zhu W, Lin C-J, Wang X, Sommar J, Fu X, Feng X (2016) Global observations and modeling of atmosphere–surface exchange of elemental mercury: a critical review. *Atmos Chem Phys* 16(7):4451–4480. <https://doi.org/10.5194/acp-16-4451-2016>

Publisher's note Springer Nature remains neutral with regard to jurisdictional claims in published maps and institutional affiliations.